JP Journal of Heat and Mass Transfer
Volume 8, Number 1, 2013, Pages 69-98
Published Online: July 2013
Available online at http://pphmj.com/journals/jphmt.htm
Published by Pushpa Publishing House, Allahabad, INDIA

A COMPARISON OF UPWINDING AND SYMMETRY CONVECTION SCHEMES FOR THE RESOLUTION OF N-S EQUATIONS

Peng Ding and Dong-Liang Sun

College of Storage and Transportation and Architectural Engineering
China University of Petroleum (Hua Dong)
Qing Dao, 266555 ShanDong, P. R. China
e-mail: ztdep@yahoo.com.cn

State Key Laboratory of Alternate Electrical Power System
with Renewable Energy Sources
North China Electric Power University
Beijing 102206, P. R. China

Abstract

This article presents a comparison of upwinding and symmetry convection schemes for the solution of the Navier-Stokes equations. The driven cavity flow problem at Reynolds number of 5000, 75000 and 10000 are solved by three different convection schemes, CD, QUICK and third order symmetry (TS), respectively. All the convection schemes are implemented on a uniform gird system with the grid density as high as 256×256. The computed results with the TS scheme are compared with the benchmark solutions and those of CD and QUICK schemes in the averaged relative error and local relative error sense. It is found the TS scheme can provide more accurate results than the QUICK scheme at the same computation cost.

Keywords and phrases: third order symmetry, convection scheme, driven cavity flow, high Reynolds number.

Communicated by K. K. Azad

Received November 23, 2012

1. Introduction

In the context of finite volume method, the discretization of the convection term in the Navier-Stokes equation or the convection-diffusion equation has been the focus of the study for more than three decades. In the early days, the central difference was used for the discretization of convection term, very accurate and stable results can be obtained only for the low Reynolds number flow, however, non-physical results will present when the cell Peclet number exceeds a certain value [1-5]. As such, various other convection schemes have been designed to obtain realistic results at high Reynolds numbers. Among the schemes used are the first order upwind (FUD), the exponential, the power-law [1] and the hybrid schemes [6].

The introduction of the “upwinding” made a major step forward in the CFD/HNT area. It was first put forward by Courant et al. [7] and subsequently by Gentry et al. [8], Barakat and Clark [9] and Runchal and Wolfshtein [10]. The upwinding scheme approximates the value of dependent variable at the control volume face more physically, the value of dependent variable at the control volume face receives more information from the upwind direction rather than an average of the two neighboring points used in the CD scheme. The first order upwind (FUD) scheme is the first used upwinding scheme in the simulation of the high Reynolds flow, it is absolute stable and bounded.

The exponential scheme [1] uses the exact solution of one-dimensional convection-diffusion problem with a Dirichlet boundary condition as the profile between two grid points. The exponential scheme achieves the stability of the upwind method and also has better accuracy. The temperature profile between grid points is linear for small *Re* and is nearly constant for large *Re*. In this limit, the exponential method approaches the interpolation rules used for central difference scheme at small Reynolds number, and first upwind scheme at large Reynolds number. The scheme is not widely used because it is expensive to compute and the schemes are not exact for two- or three-dimensional problems, nonzero source terms, etc.

The hybrid schemes are first proposed by Spalding [6], the name hybrid indicates that it is a combination of the FUD and CD schemes. It is identical with the CD scheme for Reynolds number range $-2 \leq \text{Re} \leq 2,$ it switches from CD to FUD when Reynolds number outsides this range.

The power-law scheme [1] is a computationally efficient approximation of the exponential scheme. The power-law scheme uses a power-law variation profile Reynolds number range $-10 \leq \text{Re} \leq 10,$ and it becomes identical with FUD when the *Re* outsides this range. For further detail about these schemes see Patankar and Spalding [11] and Raithby and Torrance [12].

Leonard and Drummond [13] pointed out that the preceding convection schemes including the exponential, the power-law and the hybrid schemes are essentially the same with the FUD scheme when the Reynolds number. So these schemes are all be regarded as low order schemes. These low order convection schemes have been wildly used for the simulation of convection heat transfer problems because there robustness and resulting physically realistic solutions.

However, it was shown that the FUD scheme is only first-order accurate in the sense of Taylor series truncation error sense, the leading terms of FUD behave as another diffusion term in the governing equations, which cause the distribution of the physical variables to smeared. This phenomenon has been reported by many works [14-25] and is referred as false diffusion. The false diffusion can be large enough to give physically incorrect results at high Reynolds number flows.

As discussed by Patankar [1], Davis and Mallinson [20], false diffusion is a multi-dimensional phenomenon, when the velocity vector is more than marginally skewed to the grid line, the false diffusion may become so large as to obscure the effects of physical diffusivity on the flow. In addition, Raithby [17] and Leonard [18] have shown that the presence of source term may also cause large errors when the FUD was used for the convection term. These conditions may prevail in the case of recirculating flows.

For example, in the pioneer work of Allen and Southwell [23], the problem of flow around a cylinder was solved with the FUD scheme, it was found that the downstream eddies are too short and vary little when *Re* changed from 100 to 1000. In the classical work of Leonard and Drummond [13], the Smith-Hutton problem which solves a two-dimensional steady state convection-diffusion of a scalar field in a specified velocity field. The results shown that the predicted variable profile at the outlet was serious diffused with the power-law scheme. Another more complex problem of natural convection in a rectangular cavity was solved with FUD, hybrid and the power-law convection schemes, at Grashof number 9500, both three low-order convection schemes cannot identify the 9 eddies in the center of the cavity.

The remedy methods to overcome the ‘false diffusion’ can be classified into three directions, one is to use a very fine grid system which is not practical especially for the three-dimensional problem. The second way is to take the velocity vector into account since the false diffusion is a multi-dimension phenomenon, one such scheme is the skew upwind differencing scheme of Raithby [26] which was named as skew upwind differencing. The skew upwind differencing scheme although is only first-order in, results in an impressive reduction in the false diffusion.

The third direction is to construct higher order upwinding schemes. In the sense of the third way, many convection schemes using the ‘upwinding’ idea have been developed. For example, the quadratic upstream interpolation for convective kinetics (QUICK) scheme of Leonard [27], the QUICK scheme employs a three points upstream weighted quadratic interpolation technique to approximate the variation of the physical variable between grid points. The studies from Shyy [14], Raithby [17], Leonard [18], Arampatzis and Assimacopulos [21] and Patel et al. [22] have shown that the QUICK scheme has greater formal accuracy than the conventional CD scheme and other low order scheme and retains the basic stable convective sensitivity property.

Other high order schemes include the cubic upwind interpolation (CUI) of Agarwal [28], the SMART of Gaskell and Lau [29], the SHARP of Leonard [30] and the HLPA of Zhu [31].

All these high order convection schemes use two nodes in the upwinding direction and one node in the downstream direction. In the work of Jin and Tao [32, 33], a third order symmetry scheme was proposed. The TS scheme has the same number and sort grids as the existing second-order difference scheme in the matrix created by discretization equation, but its grids constituting the scheme are symmetrical from two sides of the interface. In this paper, the performance of the TS scheme, CD scheme, and QUICK scheme was assessed by solving the driven cavity problem at high *Re* number.

2. Mathematical Formulations

2.1. Governing equations

Fluid flow and heat transfer are the predominant processes in many industry problems which are governed by a series of partial differential equations, e.g., Navier-Stokes equation for the flow field, energy equation for the temperature field and convection-diffusion equations for other scalar variable fields. In this paper, we only consider steady problems, in the finite volume method, all these governing equations can be expressed in a general convection-diffusion form [1],

$$div(\rho \boldsymbol{u} \phi) = div(\Gamma \, grad \; \phi) + S_\phi, \tag{1}$$

where $\boldsymbol{u}$ is the velocity vector, ϕ represents different dependent variables and Γ is the diffusion coefficient, it has different meaning for different dependent variables. In equation (1), the first term is called the *convection term*, the second term is called the *diffusion term* and the third term S_ϕ is called the *source term*.

With the finite volume approach, the computation domain is first discretized into a set of control volumes. A control volume in a two-dimensional discretized domain is shown in Figure 1. Integration of equation

(1) over the control volume shown gives

$$\int_{\Delta V} div(\rho \boldsymbol{u}\phi)\, dA = \int_{\Delta V} div(\Gamma\, grad\ \phi)\, dV + \int_{\Delta V} S_\phi \Delta V. \tag{2}$$

We focused on the main grid point *P* as shown in Figure 1, its neighboring nodes are *W*, *E*, *S* and *N*. The control volume faces are denoted by *w*, *e*, *s* and *n*, respectively.

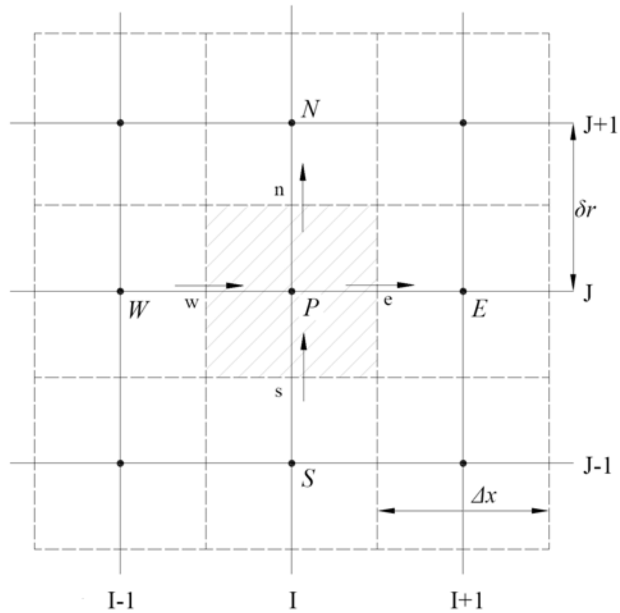

Figure 1. Control volume used for the discretization of governing equation.

Using the Gaussian divergence theorem, we obtain

$$\int_A n \cdot (\rho \boldsymbol{u}\phi)\, dA = \int_A n \cdot (\Gamma\, grad\ \phi)\, dA + \int_{\Delta V} S_\phi \Delta V. \tag{3}$$

Reformulating equation (3) in a two-dimensional Cartesian coordinate, we obtain

$$(\rho u A\phi)_e - (\rho u A\phi)_w + (\rho v A\phi)_n - (\rho v A\phi)_s$$

$$= \left(\Gamma A \frac{\partial \phi}{\partial x}\right)_e - \left(\Gamma A \frac{\partial \phi}{\partial x}\right)_w + \left(\Gamma A \frac{\partial \phi}{\partial y}\right)_n - \left(\Gamma A \frac{\partial \phi}{\partial y}\right)_s + S_\phi \Delta V. \tag{4}$$

This discretized equation represents the flux balance in a control volume, the value of the dependent variable ϕ at the control volume faces is approximated by different interpolation schemes. For the diffusion terms, central difference was used to approximate the value of the dependent variable ϕ at the control volume faces

$$\left(\Gamma A \frac{\partial \phi}{\partial x}\right)_e = \frac{\Gamma A}{\Delta x}(\phi_E - \phi_P), \qquad \left(\Gamma A \frac{\partial \phi}{\partial y}\right)_n = \frac{\Gamma A}{\Delta y}(\phi_N - \phi_S). \tag{5}$$

It is unnecessary to use high order scheme higher than second order for the diffusion term, because under high convection, the diffusion term is not very important, it is the convection term playing a key role. For the convection term, it seems logical to use the central difference scheme again. In the central difference scheme, the value of dependent variable ϕ at the control face is approximated by the average of its two neighboring nodes

$$\phi_e = (\phi_E + \phi_P)/2, \tag{6}$$

$$\phi_w = (\phi_W + \phi_P)/2. \tag{7}$$

We define two variables F and D to represent the convection mass flux and the diffusion conductance at the control volume face. Now, equation (4) can be written as

$$\frac{F_e}{2}(\phi_P + \phi_E) - \frac{F_w}{2}(\phi_P + \phi_W) + \frac{F_n}{2}(\phi_P + \phi_N) - \frac{F_s}{2}(\phi_P + \phi_S)$$

$$= D_e(\phi_E - \phi_P) - D_w(\phi_P - \phi_W) + D_n(\phi_N - \phi_P) - D_s(\phi_P - \phi_S) + S_\phi. \tag{8}$$

With the symbols of Patankar, we write equation (8) in the following general form:

$$a_P\phi_P = a_E\phi_E + a_W\phi_W + a_N\phi_N + a_S\phi_S + S_\phi \Delta V, \tag{9}$$

where

$$a_E = D_e - \frac{F_e}{2}, \tag{10}$$

$$a_N = D_n - \frac{F_n}{2}, \tag{11}$$

$$a_W = D_w - \frac{F_w}{2}, \tag{12}$$

$$a_S = D_s - \frac{F_s}{2}, \tag{13}$$

$$a_P = a_E + a_W + a_N + a_S. \tag{14}$$

The Taylor series truncation of the CD scheme is second order. With the CD scheme, very accurate results can be obtained when the convection of fluid is not very strong. But when the convection dominated, the coefficients a_E, a_W, a_N, a_S may take a negative value, and the rule 2 of Patankar will be violated, serious oscillation will present in the results. A stability analysis shows that the critical cell *Pe* number of the CD is only 2, due to this drawback, CD scheme is not a suitable discretization scheme for the general use, more stable convection scheme should be developed.

2.2. Different upwinding convection schemes

2.2.1. FUD scheme

In the CD scheme, the value of dependent variable ϕ at the control volume face is approximated by the average of its two neighboring nodes no matter its flow direction, the upwind convection scheme takes the flow direction into account: the value of ϕ should receive more information from its upwinding direction when the convection dominated.

The first order upwind (FUD) scheme was the most earliest convection scheme using the idea of upwind. In the FUD, the value of ϕ at the control volume face is written as

$$u_e > 0,\ \phi_e = \phi_P, \tag{15}$$

$$u_e < 0,\ \phi_e = \phi_E, \tag{16}$$

$$u_w > 0,\ \phi_e = \phi_W, \tag{17}$$

$$u_w < 0,\ \phi_e = \phi_P. \tag{18}$$

The coefficients of the discretized equation for the FUD are

$$a_E = D_e + \max(0, -F_e), \tag{19}$$

$$a_N = D_n + \max(0, -F_n), \tag{20}$$

$$a_W = D_w + \max(F_w, 0), \tag{21}$$

$$a_S = D_s + \max(F_s, 0), \tag{22}$$

$$a_P = a_E + a_W + a_N + a_S. \tag{23}$$

With the FUD scheme, all the coefficients of the discretized equations are positive and the matrix is diagonally dominated, no any ‘wiggles’ occur in the numerical simulation results. But the scheme is only first order, the accuracy of the results could be seriously affected by the ‘false diffusion’ especially when the flow direction is not aligned with the grid line or there are large gradient exist in the flow.

2.2.2. QUICK scheme

The quadratic upstream interpolation for convective kinetics (QUICK) scheme of Leonard [27] has been successfully used in the calculations. The face value of ϕ is obtained from a quadratic function passing through two upstream points and one downstream point,

$$u_e > 0,\ \phi_e = \frac{3}{4}\phi_P - \frac{1}{8}\phi_W + \frac{3}{8}\phi_E, \tag{24}$$

$$u_e < 0,\ \phi_e = \frac{3}{4}\phi_E - \frac{1}{8}\phi_{EE} + \frac{3}{8}\phi_P, \tag{25}$$

$$u_w > 0,\ \phi_e = \frac{3}{4}\phi_W - \frac{1}{8}\phi_{WW} + \frac{3}{8}\phi_P, \tag{26}$$

$$u_w < 0,\ \phi_e = \frac{3}{4}\phi_P - \frac{1}{8}\phi_E + \frac{3}{8}\phi_W. \tag{27}$$

The coefficients of the discretized equation for the QUICK is

$$a_E = D_e - \frac{3}{8}\alpha_e F_e - \frac{6}{8}(1-\alpha_e)F_e - \frac{1}{8}(1-\alpha_w)F_w, \tag{28}$$

$$a_{EE} = \frac{1}{8}(1-\alpha_e)F_e, \tag{29}$$

$$a_N = D_n - \frac{3}{8}\alpha_n F_n - \frac{6}{8}(1-\alpha_n)F_n - \frac{1}{8}(1-\alpha_s)F_s, \tag{30}$$

$$a_{NN} = \frac{1}{8}(1-\alpha_n)F_n, \tag{31}$$

$$a_W = D_w + \frac{6}{8}\alpha_w F_w + \frac{1}{8}\alpha_e F_e + \frac{3}{8}(1-\alpha_w)F_w, \tag{32}$$

$$a_{WW} = -\frac{6}{8}\alpha_w F_w, \tag{33}$$

$$a_S = D_s + \frac{6}{8}\alpha_s F_s + \frac{1}{8}\alpha_n F_n + \frac{3}{8}(1-\alpha_s)F_s, \tag{34}$$

$$a_{SS} = -\frac{6}{8}\alpha_s F_s, \tag{35}$$

$$a_P = a_{EE} + a_E + a_W + a_{Ww} + a_{NN} + a_N + a_{SS} + a_S, \tag{36}$$

where $\alpha_w = 1$ for $F_W > 0$; and $\alpha_w = 0$ for $F_W < 0$; $\alpha_e = 1$ for $F_e > 0$; and $\alpha_e = 0$ for $F_e < 0$.

The QUICK scheme takes more upwinding nodes into the calculation of ϕ and is more accurate than FUD and CD scheme. Just like the CD scheme, the main coefficients of the QUICK scheme are not guaranteed to be positive, so the QUICK is therefore conditional stable. The critical cell *Pe* number of the QUICK is $\frac{8}{3}$.

2.2.3. The third order symmetry scheme (TS)

Jin and Tao [32, 33] take the values of two nodes both at the upwind and downwind directions, the value of ϕ at the control volume face is evaluated as follows:

$$u_e > 0,\ \phi_e = -\frac{19}{72}\phi_W + \frac{9}{8}\phi_P + \frac{1}{24}\phi_E + \frac{7}{72}\phi_{EE}, \tag{37}$$

$$u_e < 0,\ \phi_e = -\frac{19}{72}\phi_{EE} + \frac{9}{8}\phi_E + \frac{1}{24}\phi_P + \frac{7}{72}\phi_W, \tag{38}$$

$$u_w > 0,\ \phi_w = -\frac{19}{72}\phi_{WW} + \frac{9}{8}\phi_W + \frac{1}{24}\phi_P + \frac{7}{72}\phi_E, \tag{39}$$

$$u_w < 0,\ \phi_w = -\frac{19}{72}\phi_E + \frac{9}{8}\phi_P + \frac{1}{24}\phi_W + \frac{7}{72}\phi_{WW}. \tag{40}$$

According to the analysis of Jin and Tao [32, 33], the TS scheme has a third order accuracy and absolutely stable but uses the same memory with that of the QUICK scheme.

2.3. Implementation method

The deferred correction technique of [17, 34, 35] was used to implement these high order convection schemes. In the deferred correction technique, all the high order convection schemes were expressed as the sum of the FUD and the difference between the high order scheme and FUD as follows:

$$\phi_e = \phi_e^{FUD} + (\phi_e - \phi_e^{FUD})^*. \tag{41}$$

The second part of the LHS of equation (41) is the correction term, it was calculated from the value of previous iteration and was implicitly added into the source term S_ϕ of equation (9). The coefficients a_E, a_W, a_N, a_S are the same with that of FUD scheme, through this way, both the positivity of the coefficient and diagonally domination can be assured which will enhance the stability of the solving process greatly. When the iteration converged, we will get the numerical solution with high order convection scheme. The general discretized equation with high order convection scheme can be formulated as

$$a_P\phi_P = a_E\phi_E + a_W\phi_W + a_N\phi_N + a_S\phi_S + S_\phi\Delta V + S_{dc}, \tag{42}$$

where

$$S_{dc} = F_e(\phi_e^{FUD} - \phi_e) - F_w(\phi_w^{FUD} - \phi_w) + F_n(\phi_n^{FUD} - \phi_n)$$
$$- F_s(\phi_s^{FUD} - \phi_s), \tag{43}$$

$$a_E = D_e + \max(0, -F_e), \tag{44}$$

$$a_N = D_n + \max(0, -F_n), \tag{45}$$

$$a_W = D_w + \max(F_w, 0), \tag{46}$$

$$a_S = D_s + \max(F_s, 0), \tag{47}$$

$$a_P = a_E + a_W + a_N + a_S. \tag{48}$$

3. Results and Discussions

3.1. Lid-driven cavity problem

In this section, the five convection schemes, CD, QUICK, TS were applied to the lid-driven cavity problem. The lid-driven cavity problem is often used as a test case for code verification and validation due to the simplicity of the cavity geometry and reliable benchmark solutions are readily available [36, 37].

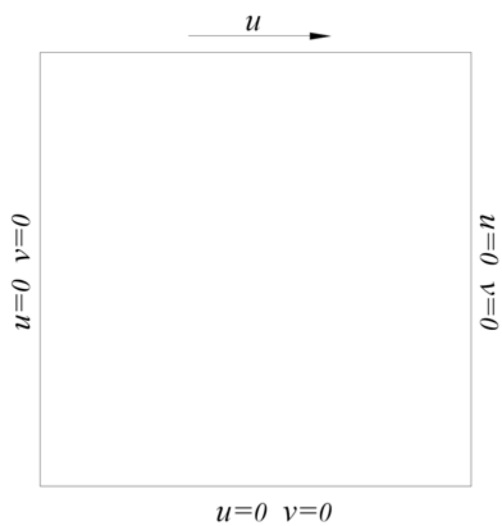

Figure 2. Control volume used for the discretization of governing equation.

Figure 2 shows a schematic view of the cavity flow and its boundary conditions. The governing equations can be written in a dimensionless form as follows:

$$\frac{\partial U}{\partial X} + \frac{\partial V}{\partial Y} = 0, \tag{49}$$

$$\frac{\partial(UU)}{\partial X} + \frac{\partial(UV)}{\partial Y} = -\frac{\partial P}{\partial X} + \frac{1}{Re}\left(\frac{\partial^2 U}{\partial X^2} + \frac{\partial^2 U}{\partial Y^2}\right), \tag{50}$$

$$\frac{\partial(UV)}{\partial X} + \frac{\partial(VV)}{\partial Y} = -\frac{\partial P}{\partial Y} + \frac{1}{Re}\left(\frac{\partial^2 V}{\partial X^2} + \frac{\partial^2 V}{\partial Y^2}\right), \tag{51}$$

where the characteristic length and characteristic velocity are the width of the cavity and the velocity of the lid, respectively.

The boundary conditions are:

$$U = 1, V = 0 \text{ on the lid,} \tag{52}$$

$$U = 0, V = 0 \text{ on the wall.} \tag{53}$$

The computational domain was discretized by three different uniform grids system, 64×64, 128×128 and 256×256. Computations were conducted at three different *Re* numbers, 5000, 7500 and 10000. According to authors' knowledge, under such great *Re* numbers and fine grid systems, the pressure correction methods such as SIMPLE [38], SIMPLEC [39] algorithms cannot give a convergent solution. In this paper, the inner doubly iterative efficient algorithm for linked equations (IDEAL) algorithm [40] was used to solve the governing equations. The convergence was declared when the normalized residual decreased to 1E-9.

Figure 3 presents the numerical simulation results for *Re* number of 5000 on a grid system of 64×64. Figure 3(a) gives the *U* velocity profile along the vertical center line of the cavity, and Figure 3(b) gives the *V* velocity profile along the horizontal center line of the cavity. The numerical simulation results of Erturk et al. [36] is also shown in the figure for comparison. In the Erturk's work, the Navier-Stokes equations in stream function and vorticity formulation were solved using a fine grid of 601×601, so the results can be treated as the benchmark solution. An overview of Figure 3 says that both the three convection schemes, CD, QUICK and TS can give physically reasonable results, but the difference between them is still very evident. The CD scheme gives the most diffusive velocity profile compared with the other two schemes, the profile departs from the benchmark solutions greatly especially at the peak values near the cavity boundary. The QUICK scheme results in more accurate results than the CD scheme, while the TS convection scheme gives the most accurate results in all these three convection schemes.

Figure 4 presents the numerical simulation results for *Re* number of 5000 on a more fine grid system of 128×128. Both the three convection schemes give more accurate results compared to those on a gird system of 64×64. But a detail examination of Figure 4 can still give the difference between the three convection scheme. Again, CD scheme give the most diffusive results, and the QUICK scheme are more accurate. The velocity profile from the TS scheme seems have collapsed onto the benchmark solution.

We further refine the grid system to 256×256 and the results were shown in Figure 5. The three schemes give the same results with the benchmark solution, little difference could be observed visually in the figure.

Figure 6 shows the comparison of the *V* velocity profile along the horizontal line passing through the center of the cavity for *Re* of 7500 at two different grid systems. Figure 6(a) gives the results on a gird system of 64×64, Figure 6(b) gives the results on a gird system of 128×128, all the results depart more from the benchmark solutions, but the overall trend is still maintained, the TS scheme gives the most accurate results, and the CD scheme gives the most diffusive results.

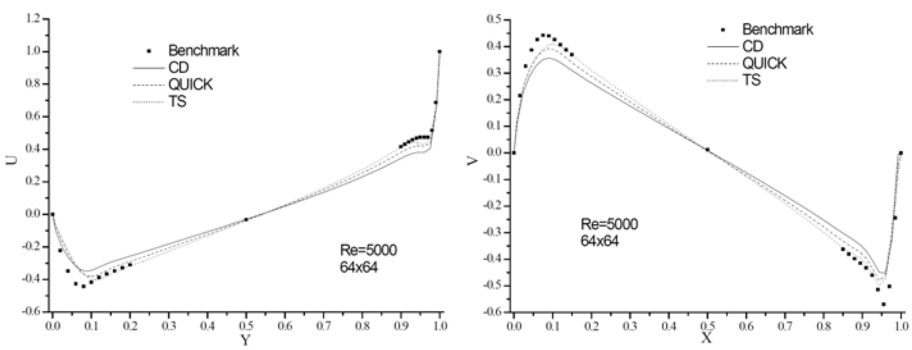

(a) (b)

Figure 3. Computed velocity along the line passing through the geometric center of the cavity at $Re = 5000$, 64×64 grid system.

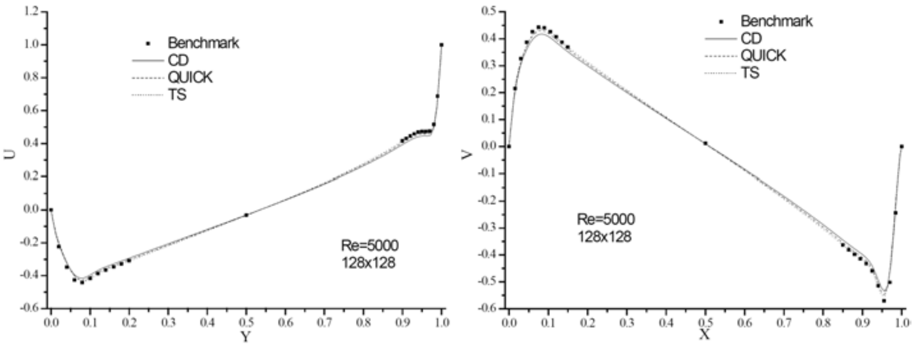

(a) (b)

Figure 4. Computed velocity along the line passing through the geometric center of the cavity at $Re = 5000$, 128×128 grid system.

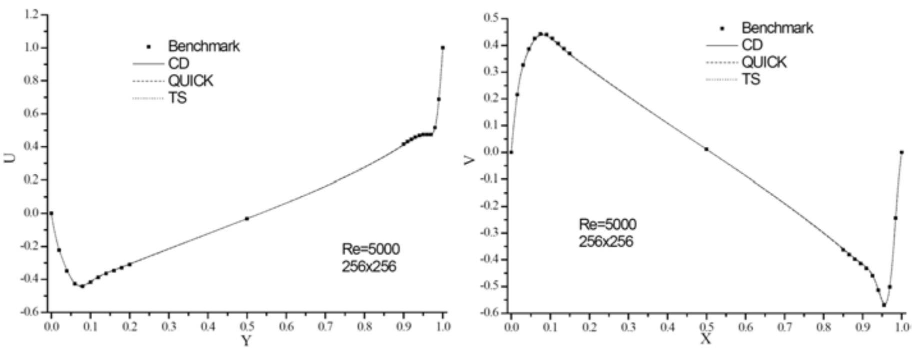

(a) (b)

Figure 5. Computed velocity along the line passing through the geometric center of the cavity at $Re = 5000$, 256×256 grid system.

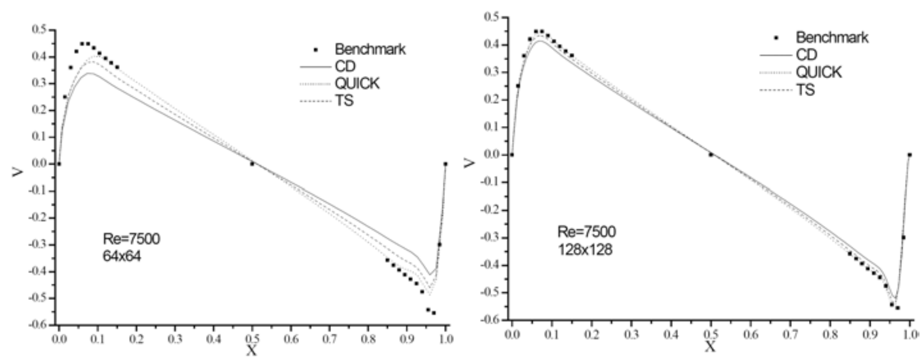

(a) (b)

Figure 6. Computed *V* velocity along the line passing through the geometric center of the cavity at $Re = 7500$.

We further increase the *Re* number to 10000, we compare the solutions in a quantitative difference sense. In this investigation, we only compare the difference for the *V* velocity since the difference between different schemes is more evident than that of *U* velocity.

We define the relative error and the averaged relative error as follows:

$$\text{Relative error } = \frac{|V - V_b|}{|V_b|} \times 100, \tag{54}$$

$$\text{Averaged relative error } = \sum_{n=1}^{N} \frac{|V - V_b|}{|V_b|} \Big/ N \times 100, \tag{55}$$

where the subscript *b* means the benchmark solutions, the variable *N* means the total number of positions where the benchmark solutions are given, it takes a value of 22. The computed results for CD, QUICK and TS schemes at three different grid systems are shown in Table 1, Table 2 and Table 3, respectively.

From the average relative error point of view, on a gird system of $64 \times 64,$ the QUICK scheme is 32% more accurate than the CD scheme, while the TS scheme is 22% more accurate than the QUICK scheme. On a gird system of $128 \times 128,$ the QUICK scheme is 33% more accurate than the CD scheme, while the TS scheme is 28% more accurate than the QUICK scheme. On a gird system of $256 \times 256,$ the QUICK scheme is 38% more accurate than the CD scheme, while the TS scheme is 33% more accurate than the QUICK scheme. At $Re = 10000,$ if a gird system of 64×64 was used with a TS scheme, the average relative error is 14.86%, to expect the same results with the CD, the mesh has to be refined to 128×128 which will be impractical in the industry.

Now we turn our attention to the relative error at certain locations as shown in the first column of tables. The maximum of the relative error occurred at the center of the cavity, it has a value of 96.93% for the TS scheme on a gird system of $64 \times 64,$ as the grid was refined to $256 \times 256,$ the value decreases to 13.86%. The same phenomenon does exist if we compare the benchmark solutions of Erturk and Ghia at the same place. At

$Re = 5000$, Ghia gave a value of 0.00945 and Erturk gave a value of 0.0117, there exits nearly 20% difference between them. At $Re = 7500$, Ghia gave a value of 0.00824 and Erturk gave a value of 0.0099, again there exists more than 16% difference between the two results.

The locations near the boundary also present a relative large relative error, since we use a uniform grid system and the FUD scheme was used for the first inner grid points. The solutions with the CD scheme take the largest error, while the results of QUICK and TS schemes are comparable. While in the other locations, the difference between these three schemes is evident, the TS scheme is at least 60% more accurate than the QUICK scheme.

Table 1. The relative error between numerical solutions and benchmark solutions at $Re = 10000$ with a 64×64 grid system (%)

X	CD	QUICK	TS
0.015	37.33	30.83	31.20
0.030	35.78	29.11	29.58
0.045	34.55	26.88	26.80
0.060	31.20	22.20	20.91
0.075	27.38	16.83	13.38
0.090	25.25	13.20	6.98
0.105	24.93	12.01	3.22
0.120	25.04	12.20	1.80
0.135	25.00	12.49	1.45
0.150	24.94	12.52	1.39
0.500	45.45	62.84	96.93
0.850	27.34	14.58	3.71
0.865	27.37	14.41	3.47
0.880	27.47	14.25	3.48
0.895	27.70	14.28	4.21
0.910	27.97	14.75	6.19
0.925	27.75	15.37	8.53

0.940	26.62	15.53	9.26
0.955	27.68	17.99	11.78
0.970	28.81	21.43	17.52
0.985	3.61	8.86	10.31
Averaged relative error	28.06	19.17	14.86

Table 2. The relative error between numerical solutions and benchmark solutions at $Re = 10000$ with a 128×128 grid system (%)

X	CD	QUICK	TS
0.015	13.23	8.11	7.04
0.030	12.09	6.57	5.49
0.045	11.81	6.18	4.55
0.060	10.57	4.74	1.79
0.075	9.53	3.57	0.75
0.090	9.16	3.30	1.69
0.105	9.26	3.56	1.39
0.120	9.44	3.78	0.93
0.135	9.52	3.84	0.81
0.150	9.56	3.89	0.83
0.500	23.98	40.62	36.65
0.850	9.44	3.36	1.36
0.865	9.47	3.41	1.37
0.880	9.50	3.45	1.41
0.895	9.65	3.59	1.28
0.910	9.91	3.97	0.61
0.925	9.78	4.26	0.41
0.940	8.00	2.66	1.04
0.955	7.34	1.35	2.59
0.970	13.97	12.51	11.84
0.985	23.23	32.47	31.27
Averaged relative error	11.35	7.58	5.48

Table 3. The relative error between numerical solutions and benchmark solutions at $Re = 10000$ with a 256×256 grid system (%)

X	CD	QUICK	TS
0.015	2.66	0.90	0.26
0.030	2.39	0.57	0.05
0.045	2.44	0.63	0.13
0.060	2.36	0.65	0.36
0.075	2.30	0.69	0.46
0.090	2.40	0.86	0.27
0.105	2.64	1.11	0.03
0.120	2.87	1.34	0.26
0.135	3.08	1.54	0.45
0.150	3.30	1.77	0.68
0.500	11.65	14.49	13.86
0.850	3.45	1.83	0.73
0.865	3.27	1.66	0.55
0.880	3.09	1.48	0.36
0.895	2.94	1.32	0.18
0.910	2.86	1.22	0.08
0.925	2.71	1.11	0.02
0.940	2.08	0.66	0.24
0.955	1.55	0.07	0.91
0.970	3.01	1.75	1.04
0.985	5.92	7.16	7.02
Averaged relative error	3.28	2.04	1.33

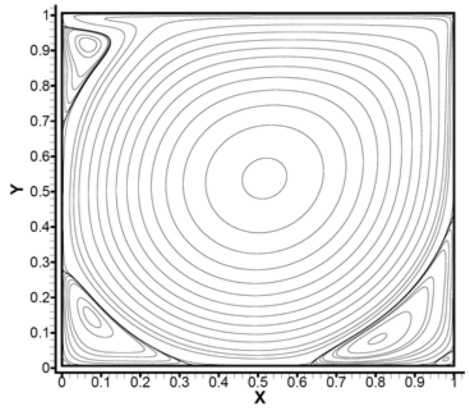

(a)

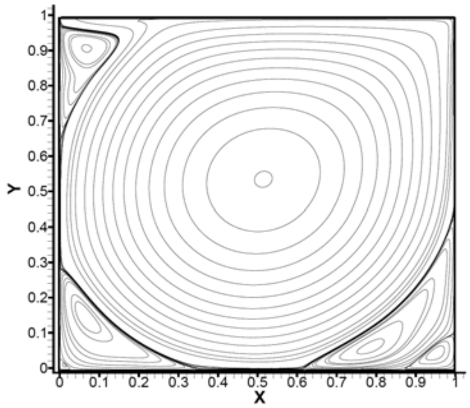

(b)

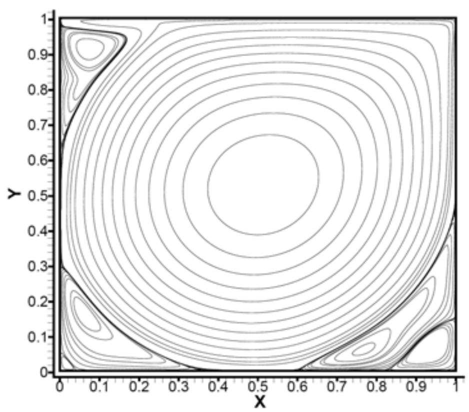

(c)

Figure 7. Streamline pattern for *Re* number of 5000, 7500 and 10000.

The streamline pattern computed with the TS scheme on a grid system of 256×256 at *Re* of 5000, 7500 and 10000 are shown in Figure 7. It is evident the second vortices at the corner of cavity increase its size as the increase of *Re* number, and the extent of vortices is in excellent agreement with the results report by Erturk et al. [36] and Ghia et al. [37].

3.2. Natural convection in a cavity

In this section, we consider the problem of natural convection of fluid in a two-dimensional cavity. Natural convection is a challenging and complex problem due to the inherent coupling of the fluid flow and the energy transport. The height *h* of the cavity is the same with the width *w* of the cavity. The fluid in the cavity is air with a constant *Pr* number of 0.71. The left wall of the cavity is kept at a constant temperature T_h, the right wall at a constant lower temperature T_c and the other two surfaces are treated as adiabatic wall.

The equations governing the flow and temperature fields are those that express the conservation of mass, momentum and energy. The flow, driven by buoyant forces, is assumed to be steady, laminar and incompressible. The fluid properties are assumed constant, except for the density in the buoyancy term, where the Boussinesq approximation is valid. The mathematical formulation for this physical problem can be written in dimensionless form as:

$$\frac{\partial U}{\partial X} + \frac{\partial V}{\partial Y} = 0,$$

$$\frac{\partial (UU)}{\partial X} + \frac{\partial (UV)}{\partial Y} = -\frac{\partial P}{\partial X} + \frac{\partial^2 U}{\partial X^2} + \frac{\partial^2 U}{\partial Y^2},$$

$$\frac{\partial (UV)}{\partial X} + \frac{\partial (VV)}{\partial Y} = -\frac{\partial P}{\partial Y} + \frac{\partial^2 V}{\partial X^2} + \frac{\partial^2 V}{\partial Y^2} + \frac{Ra}{Pr}\theta,$$

$$\frac{\partial (U\theta)}{\partial X} + \frac{\partial (V\theta)}{\partial Y} = \frac{1}{Pr}\left(\frac{\partial^2 \theta}{\partial X^2} + \frac{\partial^2 \theta}{\partial Y^2}\right),$$

where the following dimensionless parameters are introduced:

$$X = \frac{x}{w}, \quad Y = \frac{y}{w}, \quad U = \frac{uw}{\nu}, \quad V = \frac{vw}{\nu}, \quad P = \frac{pw^2}{\rho\nu^2},$$

$$\theta = \frac{T - T_c}{T_h - T_c}, \quad Pr = \frac{\nu}{\alpha}, \quad Ra = \frac{g\beta(T_h - T_c)w^3}{\nu\alpha}.$$

The parameters g, α, β and ν are the acceleration due to gravity, the thermal diffusivity of the fluid, the coefficient of thermal expansion, and the fluid kinetic viscosity, respectively.

The boundary conditions are $U = V = 0$ on all rigid walls, $\theta = 1$ at $X = 0$, $\theta = 0$ at $X = 1$ and $\partial\theta/\partial\vec{n} = 0$ on the insulation walls, wherein $\vec{n}$ means the normal direction of walls.

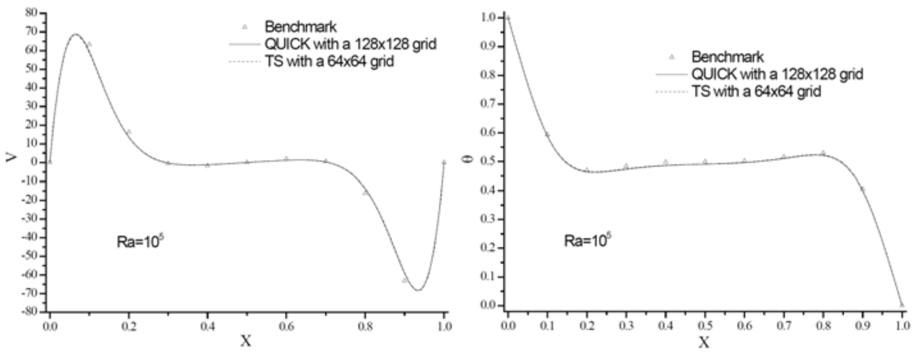

(a) (b)

Figure 8. Computed V velocity and temperature θ along the center vertical line of the cavity at $Ra = 10^5$.

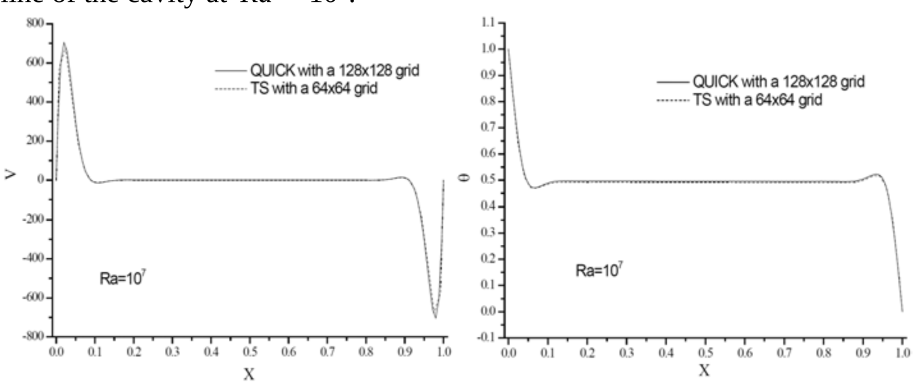

(a) (b)

Figure 9. Computed V velocity and temperature θ along the center vertical line of the cavity at $Ra = 10^7$.

Figure 8 presents the computed results at *Ra* of 10^5. Figure 8(a) shows the dimensionless *V* velocity profile along the center of the cavity, Figure 8(b) shows the dimensionless temperature profile along the center of the cavity. The benchmark solution of Wan was also shown in the figure for comparison. Wan used a high-accuracy discrete singular convolution (DSC) method for the solution of problem on a 161×161 grid system. The solid line is the results with the QUICK convection scheme on a 128×128 grid system, while the dashed line is the results with the TS convection scheme on a 64×64 grid system. An overview of Figure 8 can say that the TS convection scheme on a coarse grid almost gives the same results with the QUICK convection scheme on a fine grid.

Figure 9 give the computed results for *Ra* of 10^7, the results with the TS scheme are also in well agreement with that of the QUICK scheme.

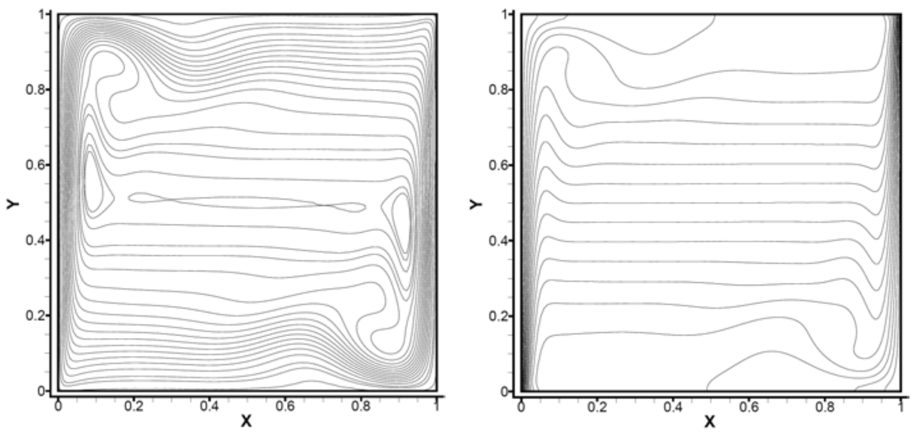

(a) (b)

Figure 10. Streamline pattern and temperature contour for $Ra = 10^7$.

The streamline pattern computed with the TS scheme on a grid system of 64×64 at *Ra* of 10^7 is shown in Figure 10. The distribution of the contour line is in excellent agreement with the results report by Wan et al. [41].

3.3. Flow over a backward facing step

Fluid flow over a backward facing step is another important benchmark problem. It has an outflow boundary condition, flow separation, flow reattachment and multiple recirculating bubbles in the channel depending on the Reynolds number and the expansion ratio. The expansion ratio is defined as the ratio of total height of the channel to the step height.

We solve the backward facing step problem at Reynolds number of 800. Figure 11 shows computed results with TS and QUICK convection schemes on different grid systems. The benchmark solutions of the Gartling [42] is also shown in the figure for comparison. We start the computation from a grid of $100 \times 20.$ We cannot obtain a convergent solution with the QUICK scheme, a 300×20 grid must be used for a fully convergent solutions. While the TS convection scheme gives an excellent prediction on a grid of 100×20 since it is unconditional stable.

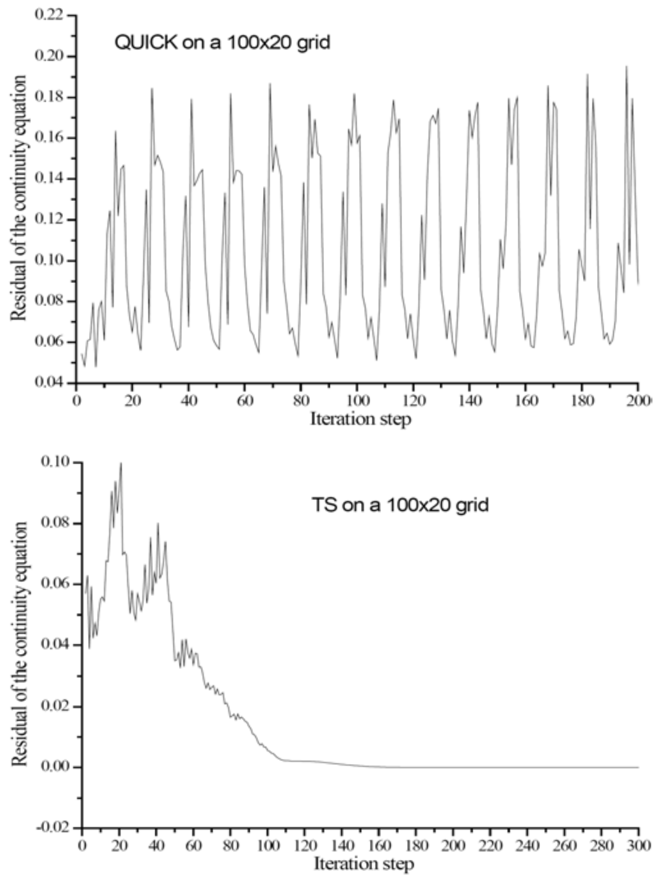

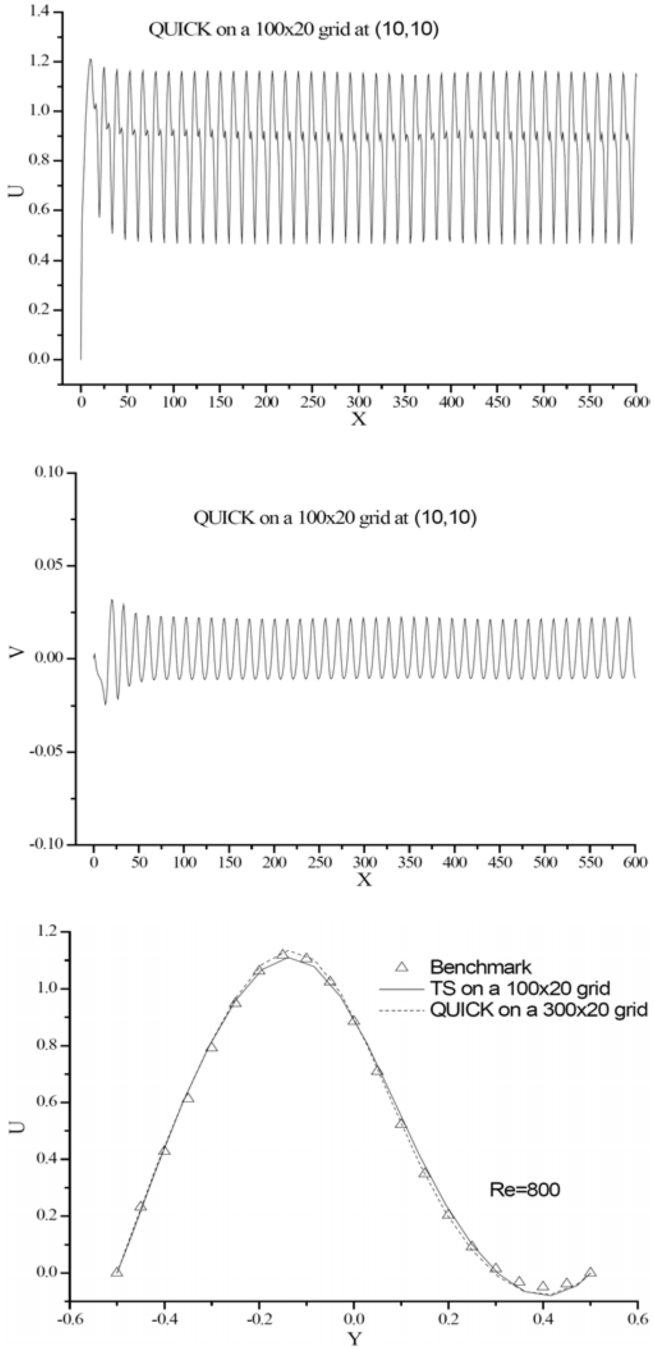

Figure 11. Computed U velocity at $X = 7.0$, $Re = 800$.

The pressure contour and the stream line are shown in Figure 12. The distribution of the pressure contour, the position of the second vortex bumble on the upper wall are in good agreement with the Gartling's results.

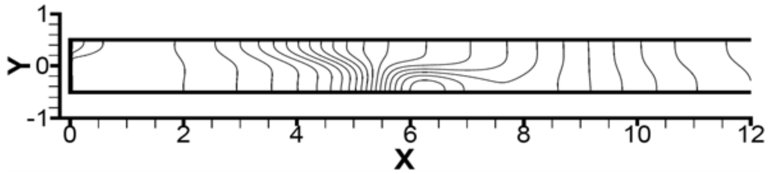

(a) Pressure contour

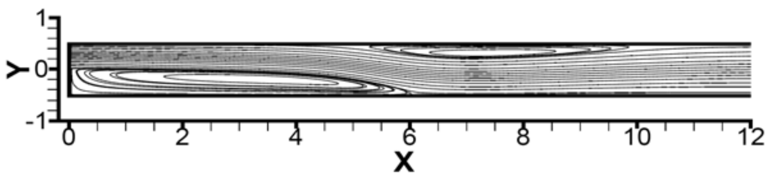

(a) Stream line

Figure 12. Streamline pattern and pressure contour for $Re = 800$ with TS.

4. Concluding Remark

A comparison has been made of upwinding and symmetry convection schemes for the solution of the Navier-Stokes equations. We have applied the CD scheme, QUICK scheme and the third order symmetry scheme (TS) to the driven cavity flow problems at Reynolds number as high as 10000. The following are some findings:

The TS scheme can provide more accurate results than the QUICK scheme.

The TS scheme resumes the same computation cost with the QUICK scheme.

The demonstrated accuracy combined with the low computational cost of the TS scheme suggests us to further extend the use of the third order symmetry scheme for the discretization of convection term especially at high Reynolds number.

Acknowledgements

This work was supported by the National Natural Science Foundation of China, Young Scientists Fund (Grant No. 51006121). This work was also partially supported by Young Scientists Fund of NSF of China (51106049).

References

[1] S. V. Patankar, Numerical Heat Transfer and Fluid Flow, Hemisphere Publishing Corporation, Taylor & Francis Group, New York, 1980.

[2] H. K. Versteeg and W. Malalasekera, An Introduction to Computational Fluid Dynamics, Addison Wesley Longman Limited, England, 1995.

[3] J. H. Ferziger and M. Peric, Computational Methods for Fluid Dynamics, Springer, Berlin, 1996.

[4] Y. Jaluria and K. E. Torrance, Computational Heat Transfer, 2nd ed., Taylor and Francis, New York, 2003.

[5] W. Q. Tao, Numerical Heat Transfer, 2nd ed., Xi'an Jiaotong University Press, Xi'an, China, 2001.

[6] D. B. Spalding, A novel finite-difference formulation for differential expressions involving both first and second derivatives, Int. J. Num. Methods Eng. 4 (1972), 551-572.

[7] R. Courant, E. Issacson and M. Rees, On the solution of non-linear hyperbolic differential equations by finite differences, Comm. Pure Appl. Math. 5 (1952), 243-254.

[8] R. A. Gentry, R. E. Martin and B. J. Daly, An Eulerian differencing method for unsteady compressible flow problems, J. Comp. Phys. 1(1) (1966), 87-118.

[9] H. Z. Barakat and J. A. Clark, Analytical and experimental study of transient laminar natural convection flows in partially filled containers, Proc. 3d Int. Heat Transfer Conf., Chicago, Vol. II, pp. 57-64.

[10] A. K. Runchal and M. Wolfshtein, Numerical integration procedure for the steady state Navier-Stokes equations, J. Mech. Eng. Sci. 11 (1980), 445-458.

[11] S. V. Patankar and D. B. Spalding, Heat and Mass Transfer in Boundary Layers, 2nd ed, Intertext Books, London, 1970.

[12] G. D. Raithby and K. E. Torrance, Upstream weighted differencing schemes and their application to elliptic problems involving fluid flow, Comput. Fluids 2 (1974), 191-205.

[13] B. P. Leonard and J. E. Drummond, Why you should not use ‘Hybrid’, ‘Power-Law’ or related exponential schemes for convective modeling – there are much better alternatives, Int. J. Numer. Meth. Fluids 20(6) (1995), 421-442.

[14] W. Shyy, A study of finite difference approximations to steady-state, a convection-dominated flow problem, J. Comp. Phys. 29 (1985), 415-438.

[15] J. D. Bozeman and C. Dalton, Numerical study of viscous flow in a cavity, J. Comp. Phys. 12 (1973), 348-363.

[16] S. Y. Tuann and M. D. Olson, Review of computing methods for recirculating flows, J. Comp. Phys. 29 (1978), 1-19.

[17] G. D. Raithby, A critical evaluation of upstream differencing applied to problems involving fluid flow, Comput. Methods Appl. Mech. Eng. 9 (1976), 75-82.

[18] B. P. Leonard, A survey of finite differences with upwinding for numerical modeling of the incompressible convective diffusion equation, Computational Techniques in Transient and Turbulent Flows, C. Taylor and K. Morgan, eds., Pineridge Press, Swansea, 1981, pp. 1-35.

[19] K. Y. Huh, M. W Golay and V. P Manno, A method for reduction of numerical diffusion in the donor cell treatment of convection, J. Comp. Phys. 63(1) (1986), 201-221.

[20] G. de Vahl Davis and G. D. Mallinson, An evaluation of upwind and central difference approximations by a study of recirculating flow, Comput. Fluids 4(1) (1976), 29-43.

[21] G. Arampatzis and D. Assimacopulos, Treatment of numerical diffusion in strong convective flows, Int. J. Numer. Meth. Fluids 18 (1994), 313-331.

[22] M. K. Patel, N. C. Markatos and M. Cross, A critical evaluation of seven discretization schemes for convection-diffusion equations, Int. J. Numer. Meth. Fluids 5 (1985), 225-244.

[23] D. N. De G. Allen and R. V. Southwell, Relaxation methods applied to determine the motion, in two dimensions, of a viscous fluid past a fixed cylinder, Quart. J. Mech. Appl. Math. 8(2) (1955), 129-145.

[24] M. A. Leschziner, Practical evaluation of three finite difference schemes for the computation of steady-state recirculating flows, Comput. Methods Appl. Mech. Eng. 19 (1979), 59-98.

[25] P. G. Huang, B. E. Launder and M. A. Leschziner, Discretizatoin of non-linear convection processes: a broad-range comparison of four schemes, Comput. Methods Appl. Mech. Eng. 48 (1985), 1-24.

[26] G. D. Raithby, Skew upstream differencing schemes for problems involving fluid flow, Comput. Methods Appl. Mech. Eng. 9 (1976), 153-164.

[27] B. P. Leonard, A stable and accurate convective modeling procedure based on quadratic upstream interpolation, Comput. Meth. Appl. Mech. Eng. 29 (1979), 59-98.

[28] R. K. Agarwal, A third-order-accurate upwind scheme for Navier-Stokes solutions at high Reynolds numbers, AIAA paper, Vol. 112, 1981, 19th AIAA Aerospace Science Meeting, St. Louis, Mo, USA.

[29] P. H. Gaskell and A. K. C. Lau, Curvature-compensated convective transport: SMART, a new boundedness-preserving transport algorithm, Int. J. Numer. Meth. Fluids 8 (1988), 617-635.

[30] B. P. Leonard, Simple high-accuracy resolution program for convective modelling of discontinuities, Int. J. Numer. Meth. Fluids 8 (1988), 1291-1305.

[31] J. Zhu, On the higher-order bounded discretization scheme for finite volume computations of incompressible flows, Comput. Methods Appl. Mech. Eng. 98 (1992), 345-359.

[32] W. W. Jin and W. Q. Tao, Design of high-order difference scheme and analysis of solution characteristics – Part I: General formulation of high-order difference schemes and analysis of convective stability, Numer. Heat Transfer, Part B: Fundamentals: An International J. Computation and Methodology 52(3) (2007), 231-254.

[33] W. W. Jin and W. Q. Tao, Design of high-order difference scheme and analysis of solution characteristics – Part II: A kind of third-order difference scheme and new scheme design theory, Numer. Heat Transfer, Part B: Fundamentals: An International J. Computation and Methodology 52(3) (2007), 255-279.

[34] T. Hayase, J. A. C. Humphrey and R. Greif, A consistently formulated QUICK scheme for fast and stable convergence using finite-volume iterative calculation procedures, J. Comp. Phys. 98 (1992), 108-118.

[35] P. K. Khosla and S. G. Rubin, A diagonally dominant second-order accurate implicit scheme, Comput. Fluids 2(2) (1974), 207-209.

[36] E. Erturk, T. C. Corke and C. Gökçöl, Numerical solutions of 2-D steady incompressible driven cavity flow at high Reynolds numbers, Inter. J. Numer. Meth. Fluids 48(7) (2005), 747-774.

[37] U. Ghia, K. N. Ghia and C. T. Shin, High-Re solution for incompressible flow using the Navier-Stokes equations and a multigrid method. J. Comput. Phys. 48 (1982), 387-411.

[38] S. V. Patankar and D. B. Spalding, A calculation procedure for heat, mass and momentum transfer in three-dimensional parabolic flows, Int. J. Heat Mass Tran. 15 (1972), 1787-1792.

[39] J. P. Van Doorman and G. D. Raithby, Enhancement of the SIMPLE method for predicting incompressible fluid flows, Numer. Heat Transfer 7 (1984), 147-163.

[40] D. L. Sun, Z. G. Qu, Y. L. He and W. Q. Tao, An efficient segregated algorithm for incompressible fluid flow and heat transfer problems – IDEAL (inner doubly iterative efficient algorithm for linked equations) Part I: Mathematical formulation and solution procedure, Numer. Heat Transfer, Part B: Fundamentals: An International J. Computation and Methodology 53(1) (2008), 1-17.

[41] D. C. Wan, B. S. V. Patnaik and G. W. Wei, A new benchmark quality solution for the buoyancy-driven cavity by discrete singular convolution, Numer. Heat Transfer B 40 (2001), 199-228.

[42] D. K. Gartling, A test problem for outflow boundary conditions-flow over a backward-facing step, Int. J. Numer. Meth. Fluids 11 (1990), 953-967.